N72-25925

NATIONAL AERONAUTICS AND SPACE ADMINISTRATION

Technical Memorandum 33-538

One Dimensional Line Radiative Transfer

K. G. Harstad

JET PROPULSION LABORATORY
CALIFORNIA INSTITUTE OF TECHNOLOGY
PASADENA, CALIFORNIA

April 1, 1972

NATIONAL AERONAUTICS AND SPACE ADMINISTRATION

Technical Memorandum 33-538

One Dimensional Line Radiative Transfer

K. G. Harstad

JET PROPULSION LABORATORY
CALIFORNIA INSTITUTE OF TECHNOLOGY
PASADENA, CALIFORNIA

April 1, 1972

Prepared Under Contract No. NAS 7-100
National Aeronautics and Space Administration

PREFACE

The work described in this report was performed by the Propulsion Division of the Jet Propulsion Laboratory.

CONTENTS

ABSTRACT

Integrations over solid angle and frequency are performed in the expressions for the radiant heat flux and local energy loss of a line in a region of strong variations of the source function in one direction. Approximations are given for coefficients and kernels in the resulting forms which involve integrals over the physical coordinate.

ONE DIMENSIONAL LINE RADIATIVE TRANSFER

INTRODUCTION

In a previous paper[(1)] the author developed an approximate expression for the local radiant energy loss of a slightly nonuniform, multidimensional, nongray, nonequilibrium plasma. The radiation source function was expanded in a Taylor series in optical depth; this series was truncated. Application of the expression developed to shock and boundary layers is therefore prohibited. The present work is complementary in that consideration is given to a narrow boundary layer region with a strong variation of the source function through the layer. The plasma core is assumed to be fairly uniform with variations taking place over lengths greater than or equal to a characteristic plasma container dimension. Its properties are assumed known; these can be obtained with aid of the expressions in the paper mentioned. Due to the physical circumstances, transverse variations in the layer can be neglected and the problem is treated as one dimensional. Although a boundary layer is examined, a shock layer would be described by similar equations.

Continuum radiation and radiation from weak lines are thin in the narrow regions considered,[1] only strong, low-level lines are likely to have thick line centers. Thus, this work is concerned only with isolated, non-thin lines. The following assumptions are utilized:

i) The radiation source function and absorption coefficient are isotropic.

ii) The container surface has diffuse emission and reflection. This assumption could be relaxed and partial specular reflection also could be considered; for many surfaces this is not necessary.[2]

iii) The intensity is isotropic at the thick line center in the plasma core. If the line center is non-thin in the layer region, it is very thick in the core. Transfer is by diffusion, gradients are not large, and this assumption should be nearly realized. It is to be noted that intensity directions near the normal to the layer are weighted favorably in the integration over solid angle.

iv) The source function and wall intensity are independent of frequency at the line center over an interval that contains the line. See references 1 and 2.

v) The impact broadening semi-half width is greater than or approximately equal to the Doppler width. This must be satisfied to use the approximations presented. Different approximations must be developed for lower pressure plasmas; this is a matter of further algebraic and computational effort. It is also assumed that the widths vary weakly through the layer.

Fluxes and the heat loss are calculated in terms of a relative normal coordinate x, x = 0 being the field point being considered. Subscript "b" will denote a boundary--either the wall or plasma core. As is customary, the positive (away from the wall) and negative (towards the wall) directions are considered separately. Two optical depths are germane to the problem: the ordinary spectral optical depth "t" and one descriptive of the line center "τ". These are given by (for either direction)

$$t = \int_o^x \alpha_\nu \, dx \tag{1}$$

and

$$\tau = \frac{1}{\left(w_\nu\big|_{x=0}\right)^2} \int_o^x K \, dx, \tag{2}$$

$$K \equiv \frac{w_\nu}{\pi} \int_o^\infty \alpha_\nu \, d\nu . \tag{3}$$

Volumetric absorption coefficient α_ν includes the effect of induced emission and w_ν is the impact semi-half width. The radiative heat flux, q_R, and volume energy loss, Q_R, are split into their backward and forward parts:

$$q_R = q_R^+ - q_R^-, \tag{4}$$

$$Q_R = Q_R^+ + Q_R^-. \tag{5}$$

Let I_b denote the intensity at a boundary and S_ν the source function, then under the listed assumptions i) through iv),

$$q_R^\pm = \pi \int_o^\infty I_b^\mp \, d\nu + 2\pi \, w_\nu\big|_{x=0} \left[\left(S_\nu\big|_{x=0} - I_b^\mp \right)\Big|_{\nu=\nu_o} C_3\left(\tau_b^\mp\right) + \int_o^{\tau_b^\mp} \Delta S_\nu \, G_2\left(\tau^\mp\right) d\,\tau^\mp \right] + \Delta q_R^\pm , \tag{6}$$

$$Q_R^\pm = \frac{2\pi K}{w_\nu}\bigg|_{x=0} \left[\left(S_\nu\big|_{x=0} - I_b^\mp \right)\Big|_{\nu=\nu_o} C_2\left(\tau_b^\mp\right) - \int_o^{\tau_b^\mp} \Delta S_\nu \, G_1\left(\tau^\mp\right) d\,\tau^\mp \right], \tag{7}$$

$\Delta S_\nu \equiv S_\nu - S_\nu\big|_{x=0}$, ν_o is the frequency at the line center,

I_b^+ is the core intensity in the normal direction,

$\Delta q_R^- = \iint \left(I_{\nu c} - I_b^+\right) \mu \, d\,\Omega \, d\,\nu$ is a correction for deviations of the core intensity $I_{\nu c}$ in the wings from being isotropic (μ is the direction cosine, Ω the solid angle), $\Delta q_R^+ = 0$ by assumption ii). The coefficient functions C_j and kernel functions G_j are given by

$$G_1 (\tau) = \frac{\left(\pi \, w_\nu \big|_{x=0}\right)^2}{w_\nu} \int_0^\infty E_1 (t) \, P_a(\nu)\big|_{x=0} \, P_a (\nu) \, d\,\nu, \tag{8}$$

$$G_2 (\tau) = \frac{\pi \, w_\nu \big|_{x=0}}{w_\nu} \int_0^\infty E_2 (t) \, P_a (\nu) \, d\,\nu, \tag{9}$$

$$C_2 (\tau_b) = \pi \int_0^\infty E_2 (t_b) \, P_a (\nu)\big|_{x=0} \, d\,\nu, \tag{10}$$

and

$$C_3 (t_b) = \frac{1}{w_\nu \big|_{x=0}} \int_0^\infty \left[\frac{1}{2} - E_3 (t_b)\right] d\,\nu, \tag{11}$$

where E_j (t) are the exponential integrals and P_a (ν) is the absorption profile, assumed to have the Voigt form. In the limit of a very thick line center ($\tau \to \infty$),

$$\begin{aligned} G_1 (\tau) &\to \frac{\sqrt{\pi}}{3 \, \tau^{3/2}} , \\ G_2 (\tau) &\to \frac{2}{3}\sqrt{\frac{\pi}{\tau}} , \\ C_2 (\tau_b) &\to \frac{2}{3}\sqrt{\frac{\pi}{\tau_b}} , \\ C_3 (\tau_b) &\to \frac{4}{3}\sqrt{\pi \, \tau_b} . \end{aligned} \tag{12}$$

The functions C_j and G_j are in general quite complex. Using the limits (12), they are written as

$$\begin{aligned} G_1 &\equiv \frac{\sqrt{\pi}}{3 \, \tau^{3/2}} F_1 (\tau) , \\ G_2 &\equiv \frac{2}{3}\sqrt{\frac{\pi}{\tau}} \, F_2 (\tau) , \\ C_2 &\equiv \frac{2}{3}\sqrt{\frac{\pi}{\tau_b}} \, F_2' (\tau_b) , \\ C_3 &\equiv \frac{4}{3}\sqrt{\pi \, \tau_b} \, F_3 (\tau_b) . \end{aligned} \tag{13}$$

For constant line widths, $F_2 \equiv F_2'$. Given in Figure 1 are the functions F_j for w_ν = constant, the Doppler width $w_D = 0$. For w_D = constant $\neq 0$, graphs of these functions relative to those of Figure 1 are presented in Figures 2 to 4. Integration over frequency was carried out numerically on a UNIVAC 1108 computer. Curves were in part verified by certain asymptotic forms and approximations. The Voigt profile is given by a rational expression with about five place or better accuracy in Ref. 3. It is seen that under assumption v), $a \equiv w_\nu / w_D \geq \mathcal{O}(1)$, the functions depend weakly on w_D, and then only for smaller τ. Note the following relations between the coefficients and kernels:

$$
\begin{aligned}
C_2(\tau_b) &= \pi - \int_0^{\tau_b} G_1(\tau)\, d\tau, \\
C_3(\tau_b) &= \int_0^{\tau_b} G_2(\tau)\, d\tau.
\end{aligned}
\tag{14}
$$

APPROXIMATIONS

Integrals (8) through (11) converge fairly slowly. Attempting numerical computer evaluation of all the integrals involved in the problem is prohibited by reasonable constraints on computer time. Quite accurate approximations in the case of constant line widths can be generated, however. Due to the relatively weak dependence on the width parameter "a", these approximations are considered useful for many applications.

For constant line widths, after integration by parts, the coefficient and kernel integrals can be rewritten as

$$
\begin{aligned}
G_1(\tau) &= \frac{\pi}{2} \Delta_1 E_1(\xi\tau) + \frac{2}{3} \xi^{3/2} W_1(\xi\tau), \\
G_2(\tau) &= \pi E_2(\xi\tau) + \frac{\pi}{2} \Delta_2 \tau E_1(\xi\tau) + \frac{4}{3} \tau \xi^{3/2} W_2(\xi\tau), \\
C_2(\tau_b) &= G_2(\tau_b), \\
C_3(\tau_b) &= \pi \tau_b E_2(\xi\tau_b) + \frac{3}{4} \pi \Delta_3 \tau_b^2 E_1(\xi\tau_b) + \frac{8}{3} \tau_b^2 \xi^{3/2} W_3(\xi\tau_b).
\end{aligned}
\tag{15}
$$

Define the function $D(\eta) \equiv \sqrt{\pi}\,\eta \exp(\eta^2) \operatorname{erfc}(\eta)$. In the above formulas (15), $\xi \equiv t/\tau\big|_{\nu=\nu_o} = D(a)$, $\Delta_1 = D(\sqrt{2}\,a)$, $\Delta_2 = 2\xi - \Delta_1$, $\Delta_3 = (\Delta_1 + 2\Delta_2)/3$, and

$$W_j(\eta) \equiv \int_o^1 \rho_j(Z,a)\sqrt{Z} \exp(-Z\eta)\, dZ \tag{16}$$

where $Z \equiv t/(\xi\tau)$ is a frequency parameter and functions ρ_j depend on the shape of the line profile. These functions have the following 'end conditions':

$$\begin{aligned} &\rho_j(0,a) = 1 \text{ and } \rho_j(1,a) = \beta_j \Delta_j/\xi^{3/2}, \\ &\beta_1 = \frac{3}{4}\pi,\ \beta_2 = \frac{3}{8}\pi,\quad \beta_3 = \frac{9}{32}\pi. \end{aligned} \tag{17}$$

Graphs of the variable end conditions are given in Figure 5. It is to be noted that the functions ρ_j are not independent, but are related by Eqns. (14). Assuming a series form for the ρ_j:

$$\rho_j = \sum_{n=0} C_n^j Z^n, \tag{18}$$

equations (14) are satisfied if

$$\begin{aligned} C_n^1 &= (1 + 2n)(1 - 2n)\, b_n, \\ C_n^2 &= (1 - 2n)\, b_n, \\ C_n^3 &= b_n. \end{aligned} \tag{19}$$

The consequent series for the W_j are

$$W_j(\eta) = \sum_{n=0} C_n^j I_n(\eta), \tag{20}$$

where $I_n(\eta) \equiv \int_o^1 Z^{n+\frac{1}{2}} \exp(-Z\eta)\, dZ$. Let $p_n \equiv 3/2 + n$. A series expansion for I_n, especially useful for $\eta \leq 1$, is

$$I_n = \sum_{k=0}^{\infty} \frac{(-\eta)^k}{k!\,(k + p_n)}.$$

For larger η, a recursion relation can be used:

$$\eta \, I_{n+1}(\eta) + \exp(-\eta) = p_n \, I_n(\eta),$$

with $$I_{-1}(\eta) = \sqrt{\frac{\pi}{\eta}} \operatorname{erf}(\sqrt{\eta}).$$

The approximation to be used for the functions (15) is to truncate the series (20). In the limit of small τ, the terms proportional to the exponential integrals dominate over the W_j terms in Eqns. (15); vice versa in the limit of large τ. The behavior of the functions ρ_j near $Z = 0$ (the line wings) is thus most important. Using an asymptotic form for the line wings, the slopes are determined:

$$b_1 = -\frac{1}{10}\xi\left(1 - \frac{3}{2a^2}\right). \tag{21}$$

The end conditions at $Z = 0$ give $b_o = 1$; the other end conditions are used to determine b_2, b_3, and b_4 with b_j assumed null for $j \geq 5$. Results are

$$\begin{aligned} -b_2 &= 6 + 3\,b_1 + \frac{99}{64}\gamma_1 - \frac{63}{32}\gamma_2\,, \\ b_3 &= 8 + 3\,b_1 + \frac{77}{32}\gamma_1 - \frac{45}{16}\gamma_2\,, \\ -b_4 &= 3 + b_1 + \frac{63}{64}\gamma_1 - \frac{35}{32}\gamma_2\,, \end{aligned} \tag{22}$$

where $$\gamma_2 = \frac{3\pi}{2\sqrt{\xi}} \text{ and } \gamma_1/\gamma_2 = \Delta_1/2\xi.$$

Table I lists the maximum deviations of this approximation from the exact functions. It should be possible to improve the accuracy by calculating b_n by use of exact numerical values of functions (15); this is not really necessary.

Consideration was given to a model problem to test the approximation developed above and also the "differential approximation" of Ref. 1 for the local heat loss. A slab of radiating medium, bounded by cold walls, is assumed to have a source distribution

$$S_\nu = S_c \cdot 2^{1+\frac{1}{m}} \frac{y^{\frac{1}{m}} (1-y)^{\frac{1}{m}}}{y^{\frac{1}{m}} + (1-y)^{\frac{1}{m}}} ,$$

where S_c is the source strength at the slab center, $y \equiv \tau/\tau_s$, and τ_s is the slab optical thickness. See Fig. 6. All necessary integrations were performed numerically on a UNIVAC 1108 computer utilizing a Romberg quadrature library subroutine. Numerical interpolation from a table of exact numerical values was used to determine the 'exact' kernels for intermediate values of τ; asymptotic expansions were used for large and small τ. The relative error control on integrations was set for a value of 10^{-4}. Library subroutines existed for the exponential integrals and error function. Calculations were performed for m = 0.5 (bell shaped distribution), m = 1 (quadratic), m = 2 (nearly flat in the slab core with a steep square root decay near a wall), and m = 4 (flat core with steeper fourth root decay near a wall); τ_s = 0.1, 1, 10, 100; a = 0.3, 3.0; and y = 0(0.1)0.5. Table II summarizes the results of the heat flux calculations (test of G_2). The approximation gives very good results, particularly for larger a.

Function G_1 is approximated with the least accuracy. For the cases $m \neq 0.5$, results of heat loss calculations are given in Table III. Again, results are good. Largest relative errors occur for small losses and the absolute error is therefore smaller. The entries of Table III for τ_s = 0.1 also hold for m = 0.5. For the case m = 0.5, at the points a = 0.3, $\tau_s \gg 1$, y = 0.2 the relative error is an order of magnitude larger than that of Table III, also it is twice as large for the point a = 0.3, τ_s = 100, y = 0.1 and for points a = 3.0, τ_s = 1, 10. A graph for m = 0.5, τ_s = 10 is given in Fig. 7; this is the case of largest deviations. It is seen that the absolute error is small. In general, the relative error for a = 3.0 is less than or equal to one quarter of that for a = 0.3.

The approximation of Ref. 1, as expected, fails to hold for $\tau_s = 0.1$ or near a wall except for the case $m = 1$, $\tau_s >> 1$. Assuming the line is totally thin is fairly accurate for $\tau_s = 0.1$ except near a wall. Overestimation of the loss in the slab core by this assumption is about 5 to 10%. Significant absorption occurs near a wall and the assumption gives large error. For $m = 0.5$, $\tau_s >> 1$, the approximation of Ref. 1 gives only order of magnitude (factor of three) agreement with exact results. This can be attributed to the importance of higher derivatives (change of curvature) of S_ν. For $m = 1$, the source function is exactly that of the truncated Taylor series and agreement is fair even for $\tau_s = 1$ where the maximum error is about 10% except near a wall where order of magnitude agreement results. For $\tau_s = 10$, maximum error is 30% ($a = 0.3$) and 10% ($a = 3.0$); for $\tau_s = 100$: 3% ($a = 0.3$, $y \neq 0$) and 1% ($a = 3.0$). Comparisons of the approximation to exact results for $m = 2,4$ are similar - it holds in the slab core where gradients are small (Fig. 8). For $\tau_s = 1$, 10 the error in the core is as large as 25% ($a = 0.3$) and 10% ($a = 3.0$). Largest error in the core is about 5% if $\tau_s = 100$.

Finally, it is to be noted that differences between the exact values of flux or loss for $\tau_s = 100$ and different a are at most about 15%.

It is suggested that an average value of a be used in problems with variations in line widths. The problem of selecting average absorption line widths is discussed in Ref. 4.

REFERENCES

1. K. G. Harstad, JQSRT 9, 1273 (1969).

2. T. R. Harrison, Radiation Pyrometry and its Underlying Principles of Radiant Heat Transfer, John Wiley & Sons, New York (1960), p. 31.

3. K. G. Harstad, submitted to J. Opt. Soc. Am.

4. K. H. Wilson and R. Greif, JQSRT 11, 1245 (1971).

TABLE I. Maximum percentage deviations of approximate $F_j(\tau,a)$ from exact values. Largest deviations occur for $1 \leq \tau \leq 10$.

a	j = 1	j = 2	j = 3
3 to ∞	0.8	0.3	0.2
1.0	1.3	0.5	0.3
0.6	2.3	0.8	0.5
0.3	5	2.7	1.4

TABLE II. Maximum percentage deviations of approximate heat fluxes from exact values for given τ_s and a.

τ_s	a = 3.0	a = 0.3
0.1	0.05	0.1
1.0	0.2*	0.2
10.0	0.2	2.1
100.0	0.1	0.7**

* Occurred at point y = 0.4 for m = 2, all other calculations give an error of 0.1% or less.

** Occurs for m = 0.5 only, all other calculations at different m give an error of 0.4% or less.

TABLE III. Maximum percentage deviations of approximate local heat losses from exact values for given τ_s and a ($m \neq 0.5$).

τ_s	a = 3.0	a = 0.3
0.1	0.1	0.4
1.0	0.2	0.7
10.0	0.5*	5.0**
100.0	0.15	1.8

* Occurred at point y = 0.1 for m = 1, all other calculations give an error of 0.3% or less.

** Occurred at point y = 0.1 for m = 1, all other calculations give an error of 2.0% or less.

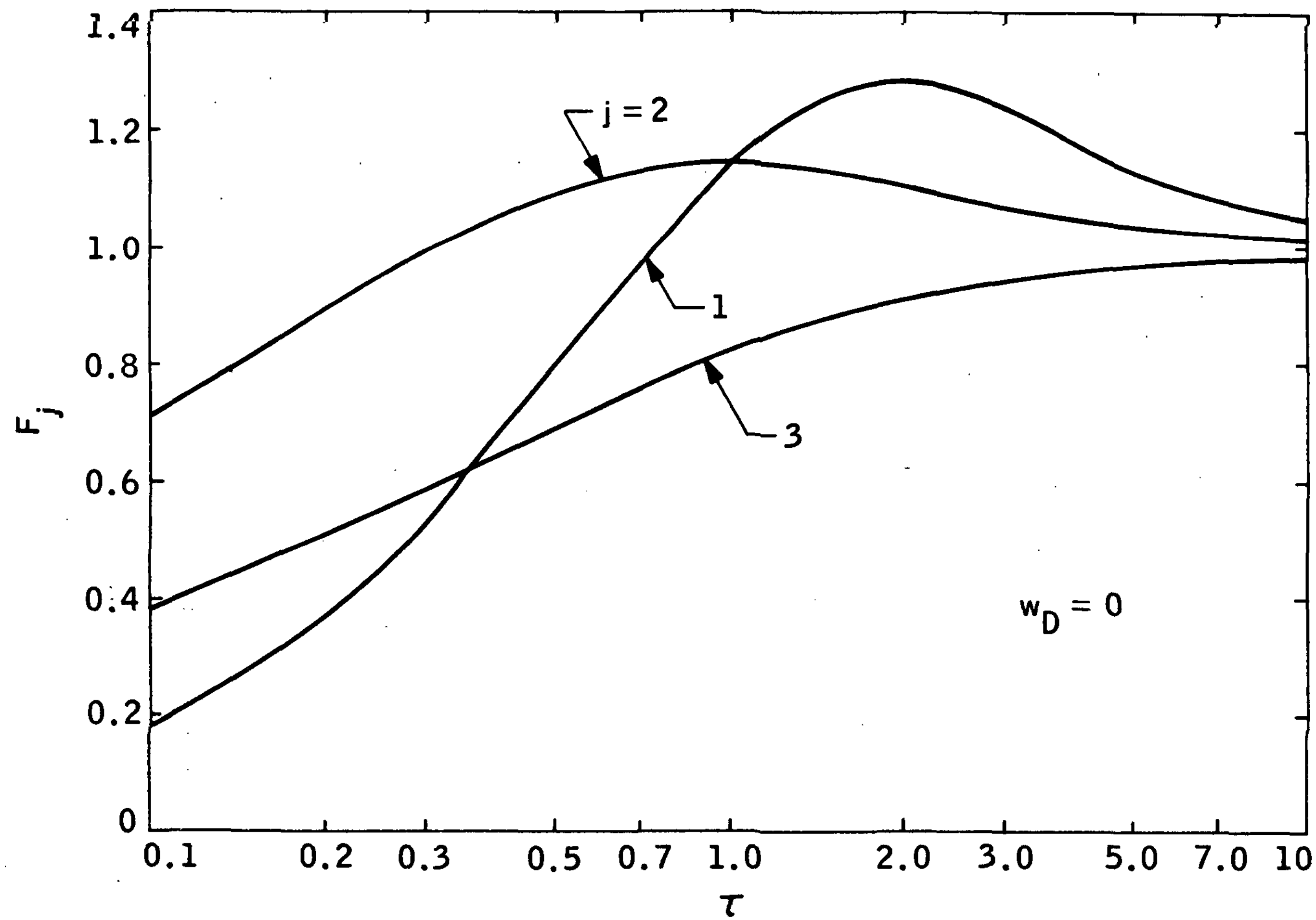

Fig. 1. Coefficient and kernel functions in the form F_j vs. τ in the limit $a \to \infty$

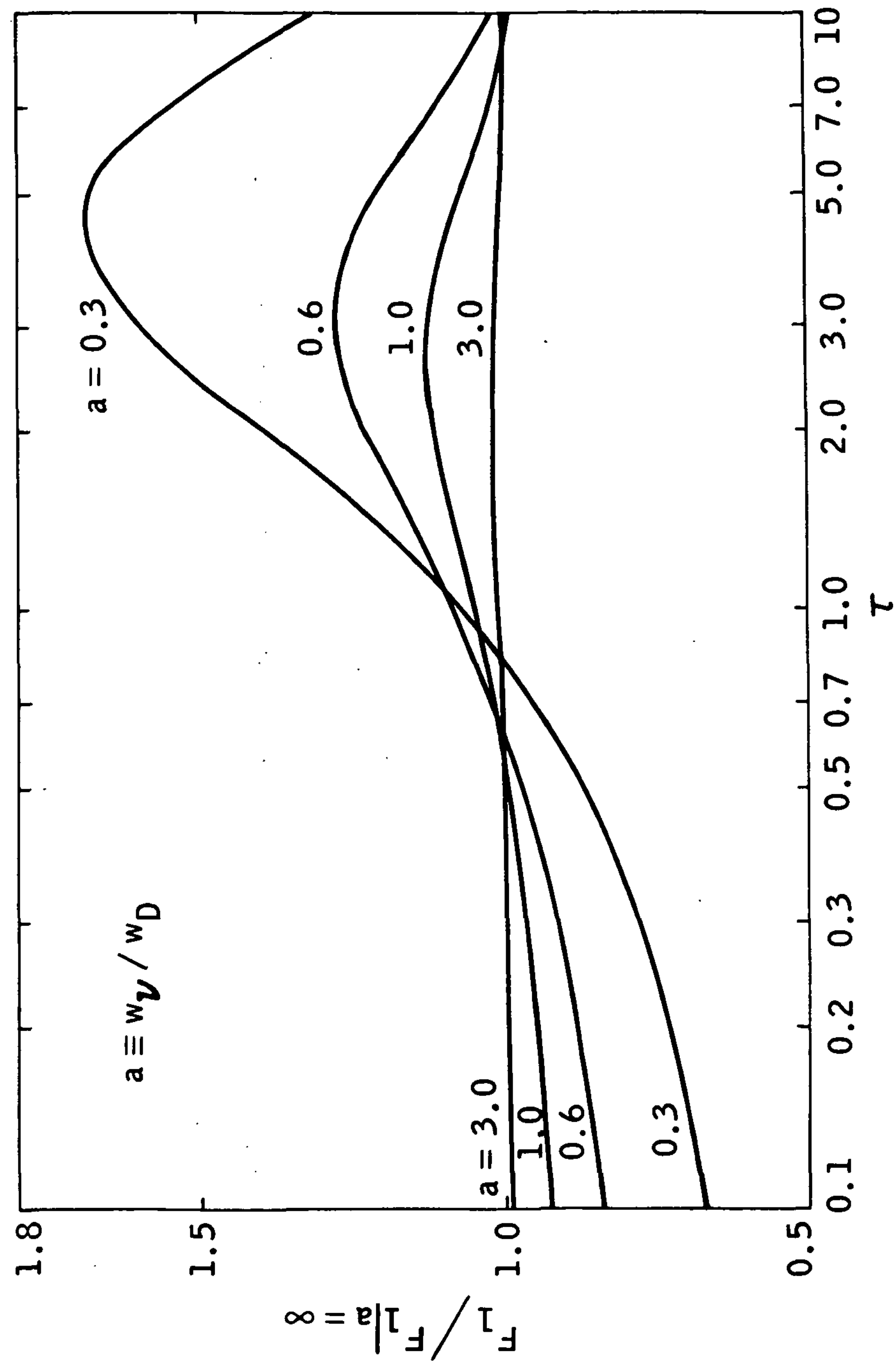

Fig. 2. Ratio of function F_1 for finite a to that given in Fig. 1

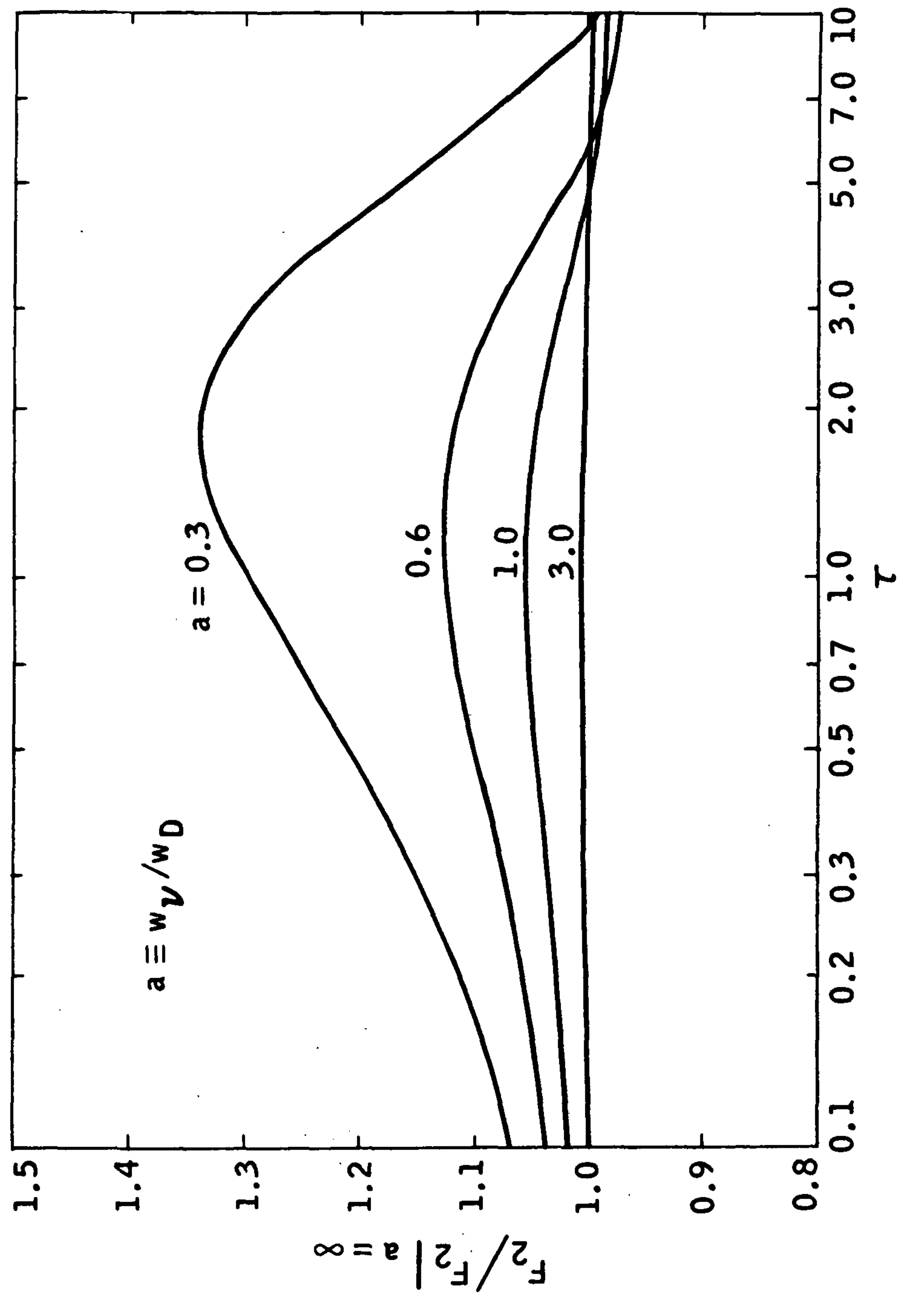

Fig. 3. Ratio of function F_2 for finite a to that given in Fig. 1

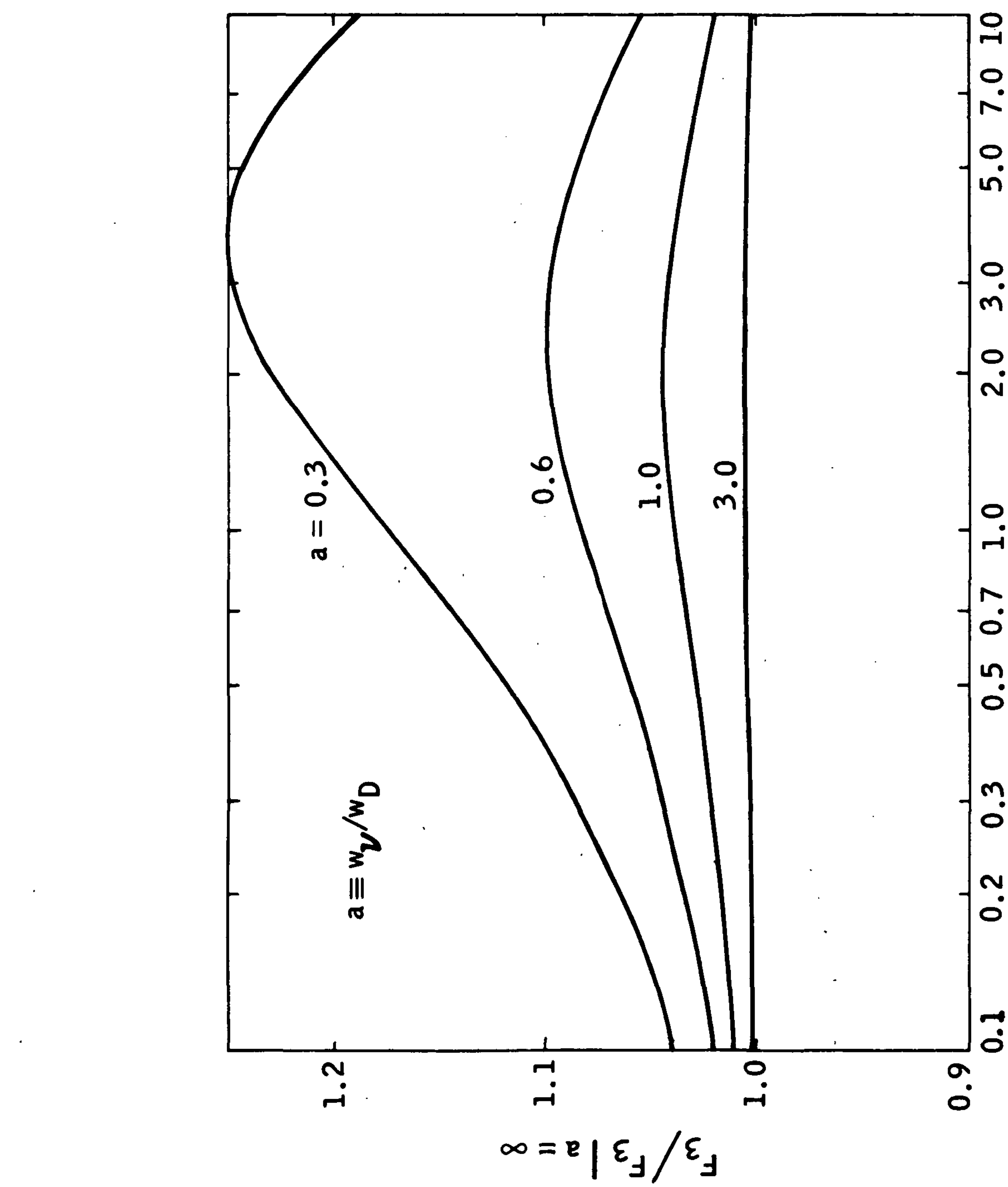

Fig. 4. Ratio of function F_3 for finite a to that given in Fig. 1

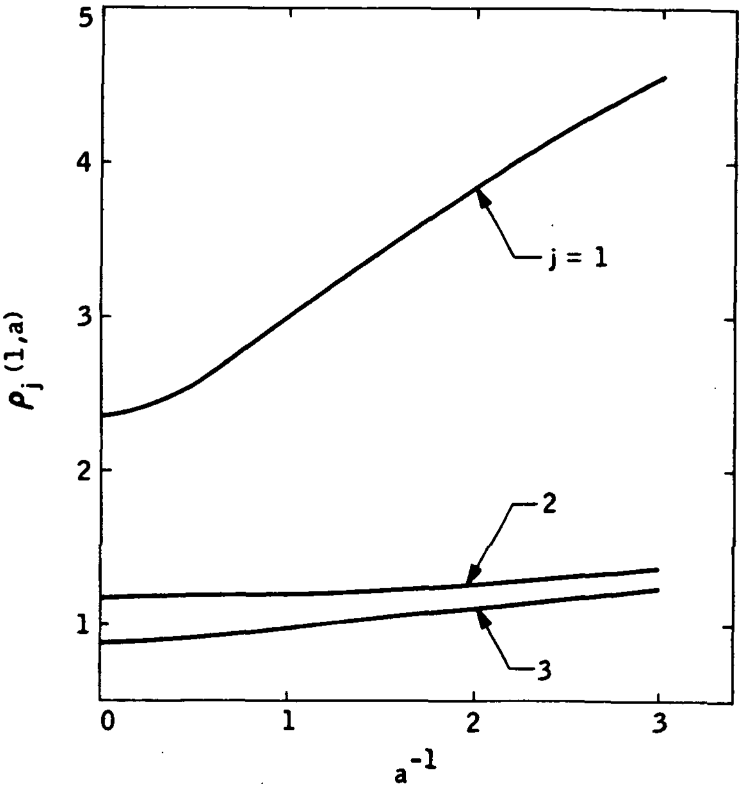

Fig. 5. The end conditions $\rho_j\,(1, a)$ for the profile functions vs. a^{-1}

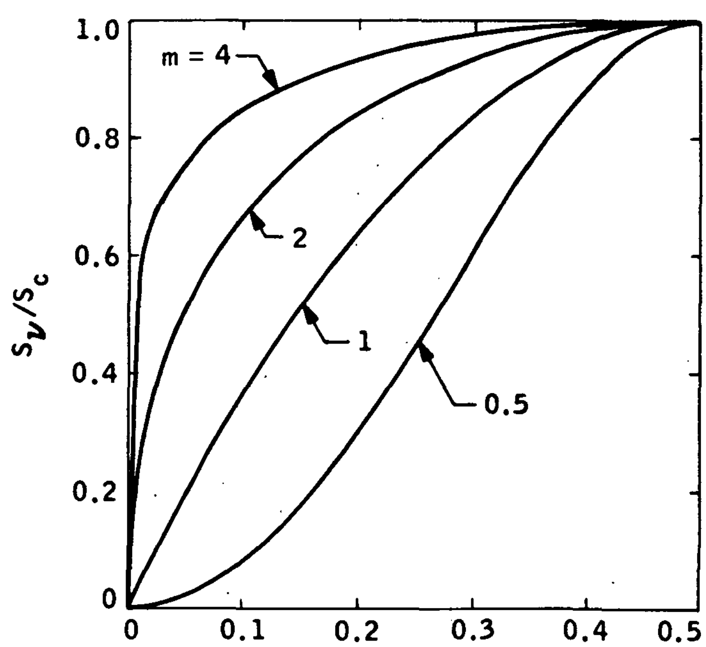

Fig. 6. Assumed line source distribution for the test model problems

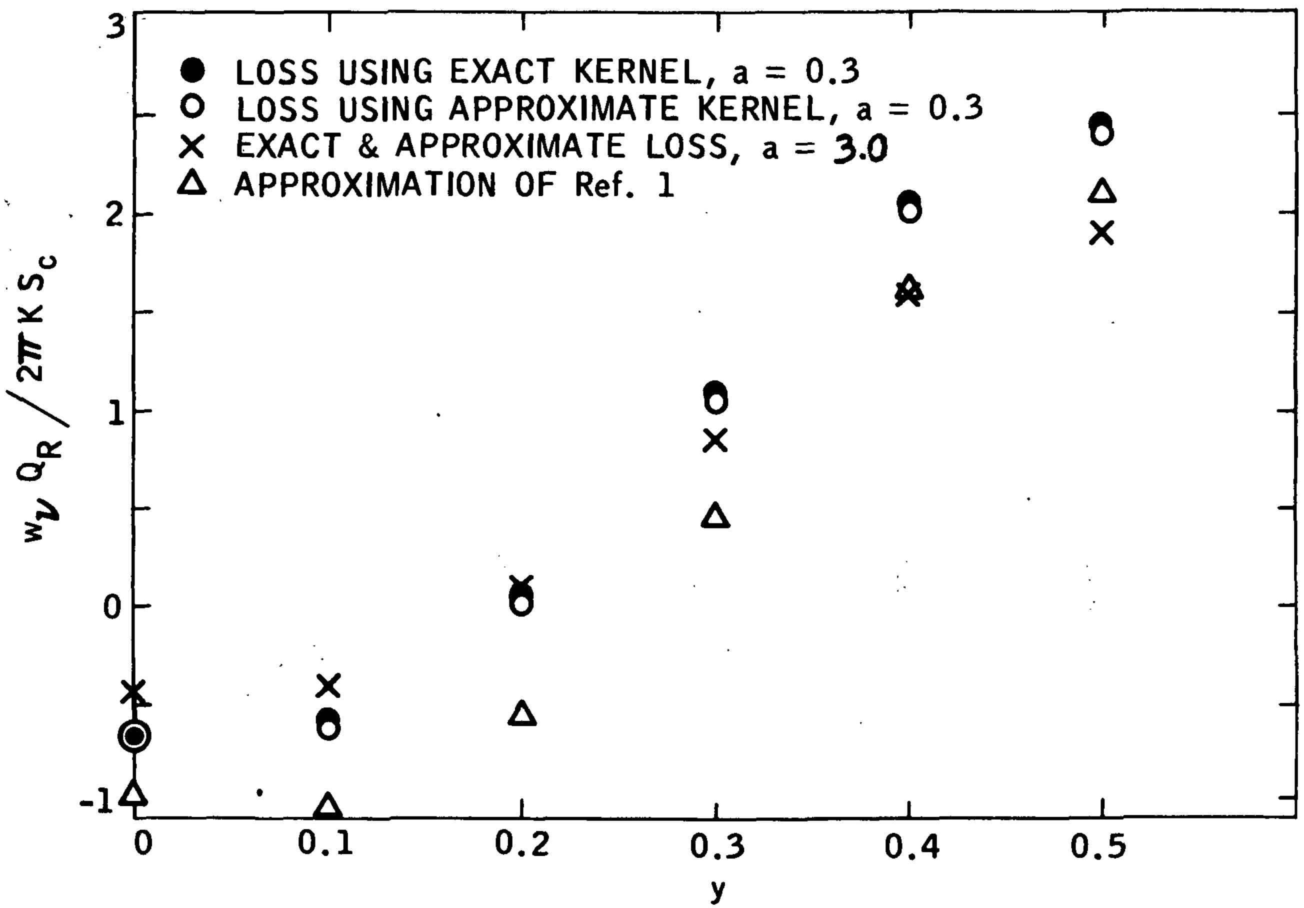

Fig. 7. Comparison of the exact local energy loss in nondimensional form to approximate losses as given here and in Ref. 1. Losses are given in terms of normalized distance y through the plasma slab for $m = 0.5$, $\tau_s = 10$ (see text)

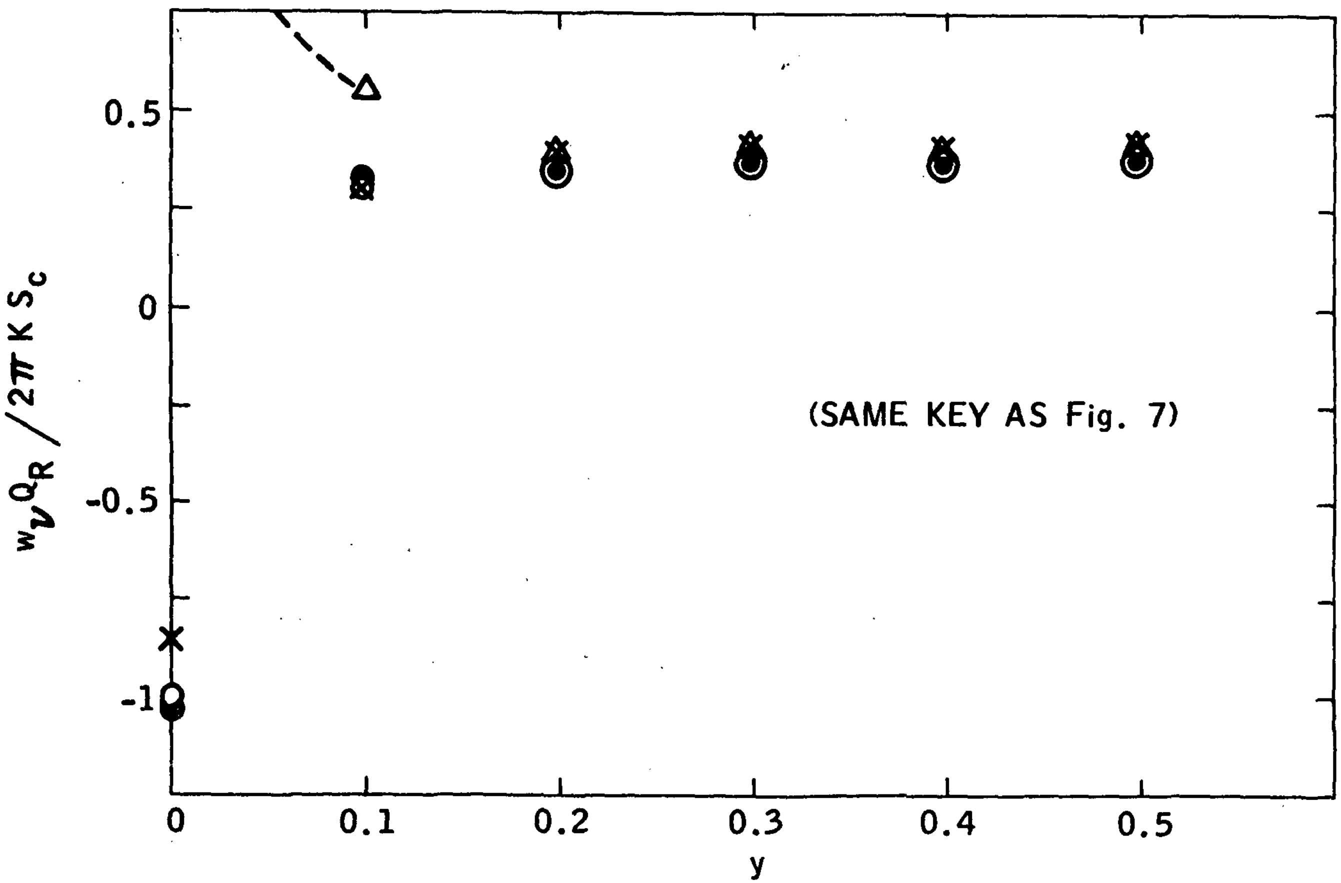

Fig. 8. Comparison of local energy losses vs. normalized distance y for $m = 2$, $\tau_s = 100$ (see text). The breakdown of the approximation of Ref. 1 in a region of large gradients is illustrated (as $y \to 0$, $Q_R \to \infty$ in this approximation).

NASA — JPL — Coml., L.A., Calif.